Available online at www.sciencedirect.com
ScienceDirect
Bioorganic & Medicinal Chemistry 16 (2008) 2077–2085
Bioorganic & Medicinal Chemistry

Corrugoside, a new immunostimulatory α-galactoglycosphingolipid from the marine sponge *Axinella corrugata*☆

Valeria Costantino,[a] Ernesto Fattorusso,[a] Concetta Imperatore,[a] Alfonso Mangoni,[a,*] Stefan Freigang[b] and Luc Teyton[b]

[a]*Dipartimento di Chimica delle Sostanze Naturali, Università di Napoli "Federico II", via D. Montesano 49, 80131 Napoli, Italy*
[b]*The Scripps Research Institute, Department of Immunology, La Jolla, CA 92037, USA*

Received 25 June 2007; revised 19 October 2007; accepted 30 October 2007
Available online 4 November 2007

Abstract—Corrugoside (**1a**), a new immunostimulatory triglycosilated α-galactoglycosphingolipid, was isolated from the marine sponge *Axinella corrugata*, and its structure determined by spectral analysis and chemical degradation. Compound **1a** activated murine NKT cells in vitro, with a potency of about 2 logs lower than that of αGalCer. Four stereoisomeric glycosphingolipids (**2a**–**2d**) were also obtained, β-glucosylceramides bearing unusual endoperoxide and allylic hydroperoxide functionalities on the sphinganine chain. They were shown to be photooxidation artifacts of the known glycosphingolipids **3**, also present in the sponge. A possible role of compound **3** as a singlet oxygen scavenger to protect the organism from oxidative damage is proposed.

1. Introduction

Sponges of the genera *Agelas* and *Axinella* are known to contain an unprecedented class of glycosphingolipids (GSLs) known as α-galactoglycosphingolipids (α-Gal-GSLs) because they are characterized by an α-galactopyranose as the first sugar of the carbohydrate chain.[2] Many α-Gal-GSLs have shown immunostimulatory properties, being able to stimulate mouse and human natural killer T (NKT).[3–5] Occurrence of α-Gal-GSLs seems to be limited to these two genera, and recent biogenetic studies reported by us[6] have suggested that their biosynthesis is not attributable to the cooperation between sponge and symbiotic microorganisms.

Further support for this chemotaxonomic association emerged from the analysis of the sponge *Axinella corrugata*, that led to the isolation of corrugoside (**1a**), a new triglycosilated α-Gal-GSL. In addition, we obtained four stereoisomeric glycosphingolipids (**2a**–**2d**), β-glucosylceramides bearing both an endoperoxide and an allylic hydroperoxide functionalities on the sphinganine chain.

2. Results and discussion

Samples of the sponge *A. corrugata* were collected along the coast of Abaco Island (Bahamas) by scuba. Freshly collected specimens were frozen on site and transferred to our lab in Napoli over dry ice. Chopped sponge was exhaustively extracted with methanol and chloroform, and the combined extracts were partitioned between water and BuOH. The organic phase was dried, and according to our standard procedure, a glycolipid fraction was obtained by subsequent reversed-phase and normal-phase column chromatography. The glycolipid fraction was acetylated, and the peracetylated glycolipids were subjected to HPLC on SiO_2 affording four fractions, composed of: (i) the known GSL **3** (25.9 mg), (ii) an inseparable mixture of compounds **2a** and **2b** (5.4 mg), (iii) an inseparable mixture of compounds **2c** and **2d** (6.8 mg), and (iv) partially purified corrugoside peracetate, **1b**. Further normal-phase HPLC purification of the last fraction gave 5.0 mg of pure compound **1b**.

Keywords: Glycolipids; Sphingolipids; Immunostimulatory activity; Marine sponges; *Axinella corrugata*.
☆ Glycolipids from sponges. 18[1]
* Corresponding author. Tel.: +39 081 678532; fax: +39 081 678552; e-mail: alfonso.mangoni@unina.it

0968-0896/$ - see front matter © 2007 Elsevier Ltd. All rights reserved.
doi:10.1016/j.bmc.2007.10.098

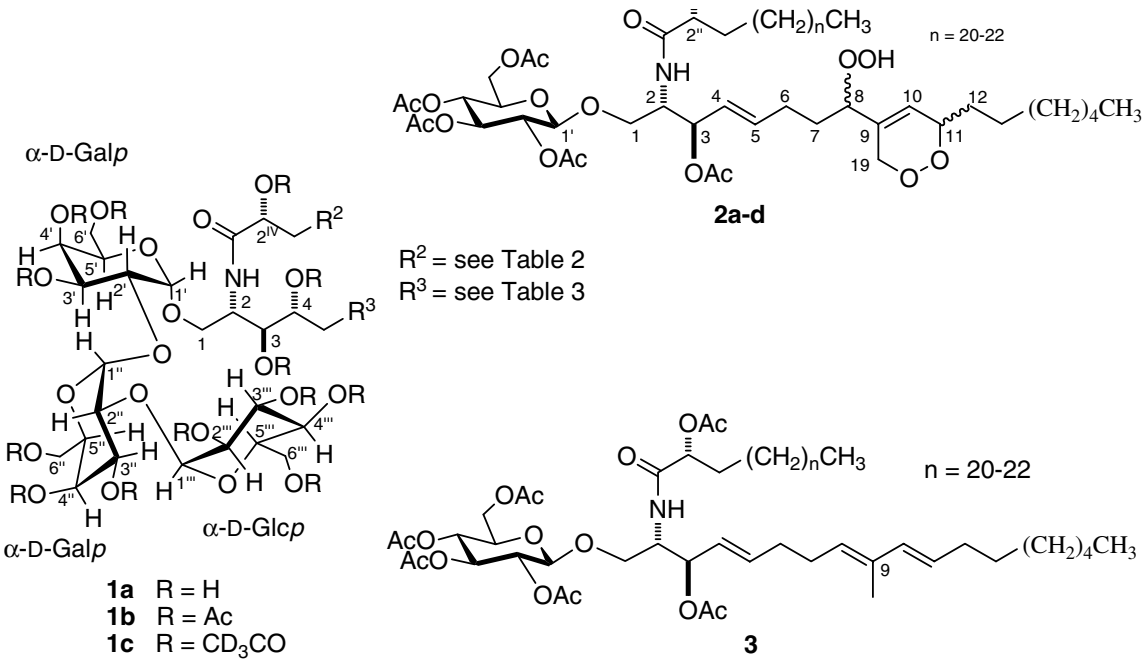

2.1. Structure elucidation of corrugoside (1a)

The ESI mass spectrum of compound **1a** showed a series of sodiated pseudomolecular ion peaks at *m/z* 1192, 1206, and 1220 in accordance with the molecular formula $C_{60}H_{115}NNaO_{20} + n\ CH_2$ ($n = 0$–2). A high-resolution measurement performed on the most abundant ion at *m/z* 1192.7918 (calcd 1192.7905) confirmed the molecular formula $C_{60}H_{115}NO_{20}$ for the dominant homologue.

A preliminary ^1H analysis of the peracetyl derivative **1b** (Table 1) in $CDCl_3$ clearly indicated its GSL nature: the intense aliphatic chain signal at δ 1.25, several signals of oxymethine and oxymethylene groups between δ 5.5 and 3.5, and a characteristic amide NH doublet at δ 7.66, suggesting the presence of the ceramide amide function. In addition, several overlapping signals were present in the methyl region of the spectrum ($\delta = 0.90$–0.83), whose intensities were not in an integral ratio with respect to those of other signals in the spectrum. This showed that the alkyl chain mixture differed not only in the length, but also in the branching of the alkyl chains.

Detailed spectroscopic analyses of **1b** in combination with chemical degradation (as described below) allowed to assess the complete stereostructure as well as the length and the branching of the alkyl chains.

The ceramide portion of molecule is that commonly found in glycolipids from marine sponges, that is, composed of a trihydroxylated, saturated sphinganine and an α-hydroxy fatty acid residue. Starting from the amide NH doublet at δ 7.48 (2-NH), all resonances of the polar part of the sphinganine up to H_2-6 were assigned through the COSY spectrum. As for the ceramide fatty acid residue, a resonance at δ 5.14 (H-2^{IV}) in the ^1H NMR spectrum of **1b**, instead of the characteristic triplet at δ 2.3 of the fatty acid α-protons, indicated the α-hydroxy substitution. This resonance showed in the ROESY spectrum an intense correlation peak with the amide NH doublet confirming the –NHCOCHOH– functionality. Both H-2^{IV} and 2-NH were shown to be coupled with the CO carbon atom at δ 170.0 (C-1^{IV}) by the HMBC spectrum.

The nature of the saccharide portion was unambiguously determined by one- and two-dimensional NMR data. The HSQC spectrum of **1b** identified resonances for the three anomeric protons (δ 5.00, 5.06, and 5.12) and the relevant carbons (δ 97.2, 97.3, and 95.4, respectively). Starting from these assignments, analysis of the COSY spectrum allowed us to assign all the proton signals of the trisaccharide moiety of **1b**. The high-field chemical shifts of H-5′ (δ 4.11), H-5″ (δ 4.45), and H-5‴ (δ 4.19) as well as the low-field chemical shifts of H-4′ (δ 5.39), H-4″ (δ 5.49), and H-4‴ (δ 5.11), indicating acetylation of the relevant OH groups, suggested the three sugars to be in the pyranose form. Analyses of coupling constants (Table 1) allowed to establish the nature of the three sugars: two sugars are galactopyranoses as evidenced by the small coupling constant between protons in position 3 and 4, the large coupling constants between protons in position 2 and 3, and by a ROESY correlation peak between the H-5 and H-3 protons for each sugar unit. The third sugar is a glucopyranose as demonstrated by the large coupling constants between all the vicinal oxymethine ring protons indicating their axial orientations. The coupling constants (all around 3.5 Hz) of each anomeric proton indicated the α stereochemistry of the three glycosidic linkages. The first sugar of the chain is an α-galactopyranose, namely the one with the anomeric proton H-1′ at

Table 1. ^{1}H and ^{13}C NMR data of corrugoside peracetate **1b** ($CDCl_3$)

Position	δ_H (mult, J (Hz))[a]	δ_C (mult)[b]
1a	3.71 (dd, 10.3, 2.8)	66.4 (CH_2)
b	3.59 (dd, 10.3, 2.7)	
2	4.33 (m)	48.5 (CH)
2-NH	7.48 (d, 9.2)	—
3	5.49 (dd, 10.1, 2.3)[d]	69.7 (CH)
4	4.86 (br. d, 10.6)	73.6 (CH)
5a	1.67 (m)	27.2 (CH_2)
b	1.56 (m)	
6a	1.36 (m)	25.8 (CH_2)
b	1.18 (m)	
1′	5.06 (d, 3.4)	97.3 (CH)
2′	3.85 (dd, 9.8, 3.4)	74.4 (CH)
3′	5.38[c]	69.5 (CH)
4′	5.39 (br. s)	68.6 (CH)
5′	4.11 (br. t, 6.4)	67.0 (CH)
6′a	4.08 (dd, 11.3, 4.7)	61.8 (CH_2)
b	4.02 (dd, 11.3, 7.2)	
1″	5.00 (d, 3.2)	97.2 (CH)
2″	3.97 (dd, 10.5, 3.2)	73.1 (CH)
3″	5.29 (dd, 10.5, 3.4)	68.4 (CH)
4″	5.49 (br. d, 3.4)[d]	68.8 (CH)
5″	4.45 (br. t, 6.3)	67.7 (CH)
6″a	4.04 (dd, 11.5, 5.4)[d]	62.2 (CH_2)
b	4.00 (dd, 11.5, 7.3)[d]	
1‴	5.12[c]	95.4 (CH)
2‴	4.93 (dd, 10.3, 3.5)	70.9 (CH)
3‴	5.45 (dd, 10.3, 9.2)	69.6 (CH)
4‴	5.11 (t, 10.3, 9.2)	68.2 (CH)
5‴	4.19 (br. d, 10.3)	67.7 (CH)
6‴a	4.26 (dd, 12.4, 3.5)	61.4 (CH_2)
b	4.05 (dd, 12.4, 2.3)[d]	
1^{IV}	—	170.0 (C)
2^{IV}	5.14 (dd, 7.5, 4.8)[d]	74.1 (CH)
3^{IV}	1.84 (m)	32.0 (CH_2)
4^{IV}	1.35 (m)	25.0 (CH_2)
Ac's CH_3	2.23, 2.16, 2.14, 2.11, 2.11, 2.10, 2.09, 2.06, 2.00, 2.00, 2.00, 1.99, 1.96	21.0–20.5 (CH_3)
CO	—	171.6–168.9 (C)

[a] Additional ^{1}H signals: δ 1.25 (broad band, alkyl chain protons), 0.88 (t, $J = 7.2$, *n*-chain Me groups), 0.86 (d, $J = 6.8$, *iso*-chain Me groups).

[b] Additional ^{13}C signals: 31.9 (CH_2, ω–2), 22.7 (CH_2, ω–1), 22.7 (CH_3, *iso*-chain Me groups), 14.1 (CH_3, ω).

[c] Overlapping signal.

[d] Overlapping signal; multiplicity and coupling constant were determined from sections of the TOCSY spectrum.

δ 5.06, because of the presence of correlation peaks of H-1′ with H-1a and H-1b in the ROESY spectrum and a correlation peak of C-1 (δ 66.4) with H-1′ in the HMBC spectrum. This sugar is glycosilated by the second galactopyranose at position 2, as demonstrated by the high-field chemical shifts of H-2′ (δ 3.85, compared with the acetylated H-2‴, δ 4.93) and by the HMBC correlation between H-1″ (δ 5.00) and C-2′ (δ 74.4). The second α-galactopyranose is glycosilated by the glucopyranose at position 2, as demonstrated by the high-field chemical shifts of H-2″ (δ 3.97) and by the HMBC correlation between H-2″ and C-1‴ (δ 95.4).

Deacetylation of **1b** with MeOH/MeONa at room temperature yielded the natural glycolipid **1a**. NMR spectra of the natural GSL **1a** were recorded and analyzed. The information provided by COSY and HMQC 2D NMR spectra confirmed all the structural features determined so far, and allowed the assignment of all the ^{1}H and ^{13}C NMR resonances of **1a** (see Section 4). The possibility that one or more of the acetyl groups in compounds **1b** were already present in the natural glycolipid was ruled out by repeating the isolation procedure after acetylation of the glycolipid fraction with trideuterioacetic anhydride instead of acetic anhydride. This gave compound **1c**, whose ^{1}H NMR spectrum was identical to that of **1b**, except that no acetyl methyl singlet was present.

Microscale chemical degradation is an essential step[7] to assess the length of the alkyl chains of a GSL when branched alkyl chains are present, because the alternative approach, that is, MS/MS analysis[8] cannot distinguish between isomeric branched and unbranched chains. Compound **1a** (100 μg) was subjected to acidic methanolysis with HCl in MeOH (Scheme 1), and the reaction products were partitioned between $CHCl_3$ and H_2O/MeOH (8:2), giving an aqueous layer consisting of methyl glycosides (fraction A) and an organic layer composed of sphinganines and fatty acid methyl esters (fraction B). Fraction A was used to determine the absolute configuration of the three sugars. The methyl glycosides were perbenzoylated with BzCl in pyridine and the reaction mixture was separated on HPLC. The chromatogram contained two peaks, that were identified as methyl tetra-*O*-benzoyl-α-D-galactopyranoside and methyl tetra-*O*-benzoyl-α-D-glucopyranoside on the basis of comparison of their retention times, ^{1}H NMR spectra, and CD spectra with those obtained from authentic samples prepared with the same procedure from, respectively, D-galactose and D-glucose.

Fraction B, containing the sphinganines and the fatty acid methyl esters from the methanolysis, was analyzed by GC–MS and was shown to contain three different unbranched 2-hydroxy fatty acid, identified by comparison of their retention times and mass spectra with those of authentic samples (Table 2). After this, fraction B was perbenzoylated as described above, and the reaction mixture was separated on normal-phase HPLC. This led to a fraction composed of 2-benzoyloxy fatty acid metyl esters (fraction C), and a fraction composed of perbenzoylated 4-hydroxysphinganines (fraction D). The CD spectra of 2-benzoyloxy fatty acid methyl esters and of perbenzoylated 4-hydroxysphinganines were used to establish the absolute configuration[7] of 2-hydroxy fatty acids and sphinganines from compound **1a** (see Section 4.4 for details).

After this, fraction D was subjected to acidic methanolysis to remove the benzoyl groups, and then to Lemieux oxidation with $KMnO_4$/$NaIO_4$ to convert 4-hydroxysphinganines to carboxylic acids with three less carbon atoms. The obtained fatty acids were methylated with CH_2N_2 and analyzed by GC–MS. The results are reported in Table 3, in the form of structures of the corresponding sphinganines.

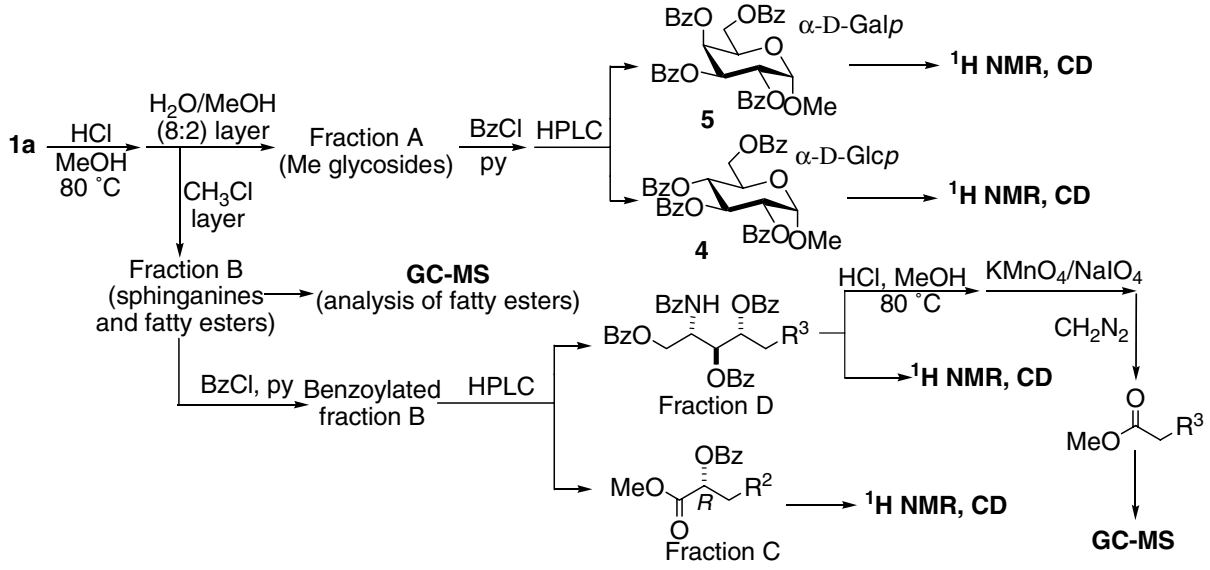

Scheme 1. Microscale degradation analysis of corrugoside (**1a**).

2.2. Immunostimulating activity of corrugoside (1a)

Corrugoside was tested for its ability to stimulate murine NKT cells in an in vitro assay using dendritic cells as antigen presenting cells and hybridoma T cells as responder cells. Corrugoside was able to stimulate Vα14 NKT cells with a potency that was about 2 logs lower than that of αGalCer, the reference agonist of NKT cells (Fig. 1). Accordingly, the in vivo injection of corrugoside did not lead to a substantial expansion of NKT cells at day 3 after injection as observed with αGalCer (data not shown). In conclusion, corrugoside is a new agonist of NKT cells.

2.3. Structure elucidation of compounds 2a–2b

In spite of our effort, we were not able to separate compounds **2a** and **2b** in any way, so they were studied as a mixture. The high-resolution ESI mass spectrum of the mixture showed three sodiated pseudomolecular ion peaks at *m/z* 1176.7036 (calcd 1176.7022), 1190.7190 (calcd 1190.7179), and 1204.7381 (calcd 1204.7335), consistent with the homologous molecular formulas $C_{61}H_{103}NO_{19}$, $C_{62}H_{105}NO_{19}$, and $C_{63}H_{107}NO_{19}$. The ^{1}H NMR spectrum was reminiscent of that of a single peracetylated GSL, except that some of the signals were doubled, suggesting the fraction to be a mixture of two compounds very similar to each other. Among them, there were several signals around δ 4.5 not commonly observed in a peracetylated GSL.

Analysis of NMR data (see Section 4.2.2) showed that the sugar portion is formed by a glucopyranose β-linked to the ceramide. In fact, all the ring protons have large coupling constants showing them to be axial. A $^3J_{CH}$ correlation between H-1′ (δ 4.11, d, J = 7.9 Hz) and C-1 (δ 67.3) confirmed the location of the glucopyranose residue on the sphinganine O-1. As for the fatty acid residue, a resonance at δ 5.35 (H-2″), instead of the characteristic triplet at δ 2.3 of the fatty acid α-protons,

Table 2. Fatty acyl composition of corrrugoside (**1a**)

Fatty acid methyl ester	
Methyl 2-hydroxyheneicosane (*n*-C_{24})	46%
Methyl 2-hydroxytetracosane (*n*-C_{25})	44%
Methyl 2-hydroxypentacosane (*n*-C_{26})	10%

Table 3. Sphinganine composition of corrugoside (**1a**)

Sphinganine	
(2*S*,3*S*,4*R*)-2-amino-1,3,4-octadecanetriol (*n*-C_{18})	83%
(2*S*,3*S*,4*R*)-2-amino-16-methyl-1,3,4-octadecanetriol (*anteiso*-C_{19})	11%
(2*S*,3*S*,4*R*)-2-amino-17-methyl-1,3,4-octadecanetriol (*iso*-C_{19})	8%

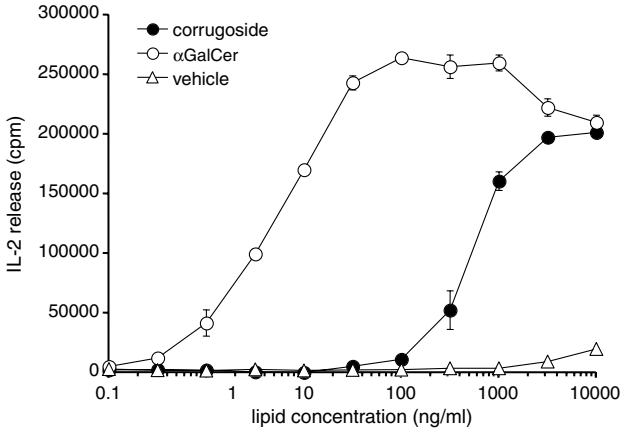

Figure 1. Corrugoside (**1a**) is presented by murine CD1d and activates NKT cells. Bone marrow-derived dendritic cells were pulsed with serial dilutions of corrugoside (closed circles), αGalCer (open circles) or vehicle (open triangles) for 4 h, washed, and used to stimulate the NKT cell hybridoma DN32.D3. Interleukin-2 concentration in supernatant after 24 h was determined in a bioassay using the proliferation of an interleukin-2 dependent cell line as readout. Means and SD of triplicates from one of two similar experiments are shown.

indicated the α-hydroxy substitution. This resonance showed an intense correlation peak with the NH doublet (δ 6.50) in the ROESY spectrum, confirming the amide function.

Structural elucidation of the sphinganine was performed through a detailed analysis of the COSY data. Starting from the amide NH signal (δ 6.50), the sphinganine spin system from C-1 to C-8 was elucidated. The amide resonance was coupled to a methine resonating at δ 4.58 (H-2), which was in turn coupled to the diastereotopic oxymethylene protons at C-1 (δ 3.79 and 3.48) and to an oxymethine proton (δ 5.54, H-3). Sequential assignments from the latter proton allowed us to assign the olefinic protons of a disubstituted double bond (δ 5.64, H-4, and 5.83, H-5), methylene protons at C-6 (δ 2.08), methylene protons at C-7 (δ 1.71 and 1.47), and the oxymethine proton at δ 4.30 (H-8). The high-field chemical shift of H-8 suggested that this oxymethine is not engaged in an ester function.

Starting from this position, chemical shifts of protons and carbons of compound **2a** were different from those of compound **2b**, indicating that the two compounds were different in this part of the molecule. However, each set of nuclei showed the same correlations in the COSY, HSQC, and HMBC spectra, suggesting that the difference was confined to the stereochemistry. In the following discussion, the reported chemical shifts refer to **2a** (chemical shifts of protons and carbons of **2b** are reported in Section 4.2.2).

The remaining two sp^2 carbon atoms in the ^{13}C NMR spectrum (one CH resonating at δ 125.9 and one non-protonated carbon at δ 136.2) and the relevant proton at δ 5.76 in the ^1H NMR spectrum provided evidence for a trisubstituted double bond. The COSY spectrum showed that the olefinic proton was coupled to H-8, to two oxymethylene protons (δ 4.73 and 4.67, H_2-19), and to an oxymethine proton at δ 4.68 (H-11), the latter being linked to the remaining part of the alkyl chain of the sphingoid base as shown by the COSY correlation peaks between H-11 and protons at C-12.

All the coupling constants were very small, and did not allow us to distinguish between vicinal and allylic couplings. However, the HMBC correlation between C-12 (δ 32.9) and the olefinic proton at δ 5.76 showed the olefinic CH to be linked to C-11, thus defining the partial structure depicted below.

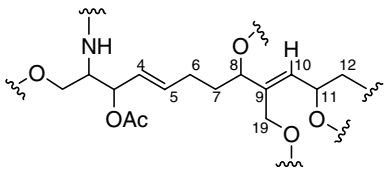

At this point, the only way to account for the remaining oxygen atom and site of unsaturation required by the molecular formula is to suppose the presence of a hydroperoxide function and a peroxide ring on the sphinganine. The location of the epoxide ring was established to be 11,19 on the basis of ROESY data. In fact, the cross-peak between H-8 and H-10, and that between one of the two protons at C-19 (δ 4.73) and both protons at C-7 was not consistent with the alternative 8,11- or 8,19-epoxide. As a consequence, the hydroperoxide function must be located at C-8.

Compounds **2a** and **2b** have the same planar structure, and may only differ in stereochemistry. Considering that differences between the NMR spectra of the two compounds are limited to signals between C-8 and C-12, they must be epimers at C-8 and/or at C-11. No attempt was made to determine the configurations at C-8 and C-11, nor to establish whether **2a** and **2b** are epimers at C-8, at C-11, or at both carbons.

Acidic methanolysis of **2a**–**2b** gave a mixture which was analyzed by GC–MS and shown to contain three different unbranched 2-hydroxy fatty acid methyl esters (C_{24}, 47%, C_{25}, 44%, and C_{26}, 9%), whose relative amounts are in the same ratio as the intensities of the pseudomolecular ion peaks in the ESI mass spectrum. This showed that the homologues only differed in the fatty acid, while the C_{18} sphinganine was identical in all the molecules.

2.4. Structure elucidation of compounds 2c–2d

The ESI mass spectrum of fraction B showed three sodiated pseudomolecular ion peaks at *m/z* 1176, 1190, and 1204 identical to those of fraction A. The ^1H NMR spectrum was also very similar, and differences were confined to the sphinganine signals (see Section 4.2.3). In addition, most of these signals were doubled, as already observed for fraction A. A set of 1D and 2D NMR spectra of fraction B were acquired, showing that

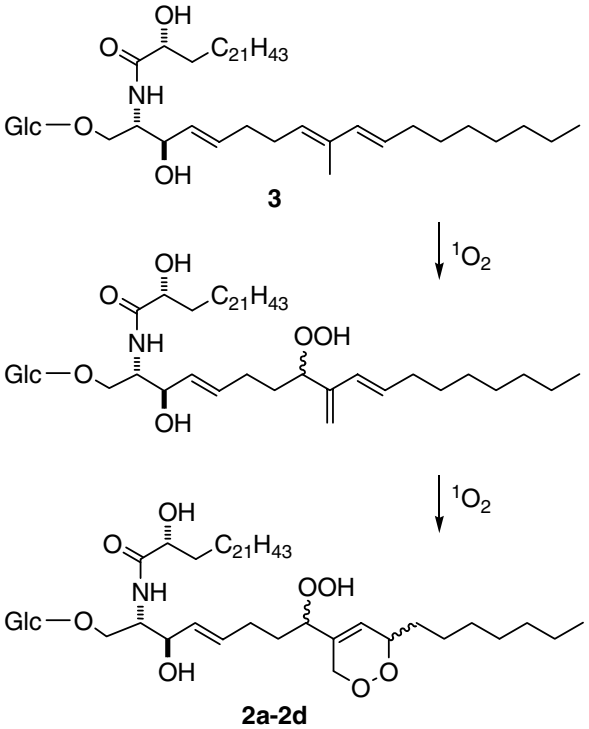

Scheme 2. Proposed mechanism of formation of compounds **2a**–**2d**.

the fraction was composed of two stereoisomers, with the same planar structure as compounds **2a** and **2b**. As a consequence, compounds **2c** and **2d** are the two remaining possible stereoisomers at C-8 and C-11 of **2a** and **2b**.

2.5. Compounds 2a–2d as photooxidation artifacts

The unusual presence of two peroxide functions on the sphinganine of glycolipids **2a**–**2d**, and the co-occurrence of all the four possible diastereomers, suggested that they could be artifacts, derived by a process of photosensitized oxidation of the GSL **3** present in the sponge. Two subsequent additions of singlet oxygen to compound **3** could account for the hydroperoxide and endoperoxide function of compounds **2a**–**2d** (Scheme 2). Although quite unusual, this mechanism has been previously described in the literature.[9]

To check this hypothesis, we repeated the extraction of the sponge, taking care to work in the dark all the time. While all the other GSLs were still present in this extract, we were not able to isolate compounds **2a**–**2d**.

3. Conclusion

The presence of corrugoside (**1a**) in *A. corrugata* confirms the ability of sponges of the genera *Agelas* and *Axinella* to synthesize a wide range of glycosphingolipids belonging to the unique class of α-Gal-GSLs. Remarkably, corrugoside is characterized by the unique triglycoside Glc(1 → 2)Gal(1 → 2)Gal which has no precedent in natural glycolipids, nor in any natural glycoconjugate. Corrugoside, like most natural α-Gal-GSLs, is an agonist of NKT cells, but its potency is much lower than αGalCer. It is known[10] that α-Gal-GSLs with a glycosylated galactose 2-OH group can stimulate NKT cells only after lysosomal processing resulting in removal of the terminal sugar(s). Thus, the lower activity is most likely due to the necessary processing of corrugoside in the lysosome to produce αGalCer, that is the stimulatory compound. Similar lower stimulation activity has been noted for all synthetic diglycosyl ceramides that we have tested. The requirement for processing for the presentation of corrugoside (cleavage of the two terminal sugars to expose the αGalCer moiety) will be explored. The lower activity could also in part be explained by a different rate of uptake of monoglycosyl versus triglycosyl in the presentation assay.

Even if the peroxide glycosphingolipids **2a**–**2d** were shown to be artifacts, their presence in the sponge can provide a hint about the function of their parent compound **3**. Glycosphingolipids with a triunsaturated sphingosine like that of **3** have been isolated for the first time from the sea star *Ophidiaster ophidiamus*,[11] and are quite common in sponges and other marine organisms, but their function is at present unknown. The ease by which compound **3** can react with singlet oxygen could suggest a possible role of these compounds as a singlet oxygen scavenger to protect the organism from oxidative damage.

4. Experimental

4.1. General experimental procedures

High-resolution ESI-MS spectra were performed on a Bruker APEX II FT-ICR mass spectrometer. ESI-MS experiment was performed on a Applied Biosystem API 2000 triple-quadrupole mass spectrometer. All the mass spectra were recorded by infusion into the ESI source using MeOH as the solvent. Optical rotations were measured at 589 nm on a Perkin-Elmer 192 polarimeter using a 10-cm microcell. ^{1}H and ^{13}C NMR spectra were determined on Varian UnityInova 700 MHz and 500 MHz NMR spectrometers; chemical shifts were referenced to the residual solvent signal ($CDCl_3$: δ_H 7.26, δ_C 77.0; pyridine-d_5: δ_H 8.71, 7.56, and 7.19; δ_C 149.9, 135.6, and 123.6). For an accurate measurement of the coupling constants, the one-dimensional ^{1}H NMR spectra were transformed at 64K points (digital resolution: 0.09 Hz). Homonuclear ^{1}H connectivities were determined by COSY and TOCSY (mixing time 100 ms) experiments. Through-space ^{1}H connectivities were evidenced using a ROESY experiment with a mixing time of 450 ms. The reverse single-quantum heteronuclear correlation (HSQC) spectra were optimized for an average $^{1}J_{CH}$ of 145 Hz. The multiple-bond heteronuclear correlation (HMBC) experiments were optimized for a $^{3}J_{CH}$ of 8 Hz. GC–MS spectra were performed on an Agilent 6850 gas chromatograph with a mass selective detector MSD HP 5975B, a split/splitless injector, and a fused-silica column, 25 m × 0.20 mm HP-5 (cross-linked 25% Ph Me silicone, 0.33-mm film thickness); the temperature of the column was varied, after a delay of 3 min from the injection, from 150 °C to 280 °C with a slope of 10 °C min^{-1}; quantitative determination was based on the area of the GLC peaks. High performance liquid chromatography (HPLC) was achieved on a Varian Prostar 210 apparatus equipped with an Varian 350 refractive index detector or a Varian 325 UV detector.

4.2. Collection, extraction, and isolation

Specimens of *A. corrugata* were collected in the summer of 2003 along the coast of Abaco Island (Bahamas) and identified by Prof. Sven Zea (Universidad Nacional de Colombia, Instituto de Investigaciones Marinas y Costeras, Invemar, Santa Marta). They were frozen immediately after collection and kept frozen until extraction. The sponge (100 g of dry weight after extraction) was homogenized and extracted with methanol (3× 1 L) and then with chloroform (3× 1 L); the combined extracts were partitioned between H_2O and *n*-BuOH. The organic layer was concentrated in vacuo and afforded 37.6 g of a dark green oil, which was chromatographed on a column packed with RP-18 silica gel. A fraction eluted with $CHCl_3$ (6.3 g) was further chromatographed on a SiO_2 column, giving a fraction [313.5 mg, eluent: EtOAc/MeOH (7:3)] mainly composed of glycolipids. This fraction was peracetylated with Ac_2O in pyridine for 12 h. The acetylated glycolipids were subjected to HPLC separation on an SiO_2 column [eluent: *n*-hexane/EtOAc (6:4)].

Four major fractions were obtained, composed of (i) the known GSL **3** (25.9 mg), whose structure was determined by comparison of its ^{1}H NMR and mass spectra with those reported,[11], (ii) a mixture of compounds **2a** and **2b** (5.4 mg), (iii) a mixture of compounds **2c** and **2d** (6.8 mg), and (iv) partially purified compound **1b** (12.0 mg). Further normal-phase HPLC purification of this last fraction [eluent: *n*-hexane/*i*-PrOH (85:15)] gave 5.0 mg of pure corrugoside peracetate (**1b**).

4.2.1. Corrugoside peracetate (1b). Colorless oil. ESI-MS (positive ion mode, MeOH) *m/z* 1738, 1752, and 1766 ([M + Na]$^+$ series) ^{1}H and ^{13}C NMR: Table 1; Composition in fatty acids: Table 2; Composition in sphinganines: Table 3.

4.2.2. Compounds 2a–2b (inseparable mixture). Colorless oil. HRESI-MS (positive ion mode, MeOH) *m/z* 1176.7036 ([M+Na]$^+$, $C_{61}H_{103}NNaO_{19}$ gives 1176.7022), 1190.7190 ([M+Na]$^+$, $C_{62}H_{105}NNaO_{19}$ gives 1190.7179), and 1204.7381 ([M+Na]$^+$, $C_{63}H_{107}NNaO_{19}$ gives 1204.7335). ^{1}H NMR of **2a** ($CDCl_3$): δ 6.50 (1H, d, J = 8.9 Hz, NH-2), 5.83 (1H, m, H-5), 5.76 (1H, br. s, H-10), 5.64 (1H, dd, J = 15.1 and 6.3 Hz, H-4), 5.54 (1H, m, H-3), 5.35 (overlapped, H-2″), 5.33 (1H, t, J = 9.8 Hz, H-3′), 5.25 (1H, t, J = 9.8 Hz, H-4′), 5.15 (1H, dd, J = 9.8 and 7.9 Hz, H-2′), 4.73 (1H, br. d, J = 15.8 Hz, H-19a), 4.68 (overlapped, H-11), 4.67 (overlapped, H-19b), 4.58 (1H, m, H-2), 4.30 (1H, br. dd, J = 8.1 and 5.1 Hz, H-8), 4.23(1H, dd, J = 12.5 and 4.0 Hz, H-6′a), 4.11 (1H, d, J = 7.9 Hz, H-1′), 4.07(1H, dd, J = 12.5, 2.2 Hz, H-6′b), 3.79 (1H, dd, J = 10.3 and 3.3 Hz, H-1a), 3.48 (1H, dd, J = 10.3 and 4.2 Hz, H-1b), 3.19 (1H, ddd, J = 9.8, 4.0, and 2.2 Hz, H-5′), 2.08 (2H, m, H_2-6), 2.02 (overlapped, H-3″a), 1.97 (3H, s, Ac), 1.96 (overlapped, H-3″b), 1.85 (3H, s, Ac), 1.81 (3H, s, Ac), 1.80 (3H, s, Ac), 1.71 (overlapped, H-7a), 1.68 (3H, s, Ac), 1.66 (3H, s, Ac), 1.61 (overlapped, H-12a), 1.47 (overlapped, H-7b), 1.47 (overlapped, H-4″), 1.43 (overlapped, H-12b), 1.32 (broad band, alkyl chain protons), 0.90 (6H, t, J = 7.0, terminal Me groups). ^{1}H NMR of **2b** ($CDCl_3$): same signals as for compound **2a**, except for δ 4.75 (1H, br. d, J = 15.8 Hz, H-19a), 4.60 (overlapped, H-19b), 4.53 (1H, m, H-11), 4.27 (1H, br. dd, J = 8.1 and 5.1 Hz, H-8), 1.75 (overlapped, H-12a), 1.49 (overlapped, H-12b). ^{13}C NMR of **2a** ($CDCl_3$): δ 170.0-168.9 (several C, acetyl CO groups), 169.8 (C, C-1″), 136.2 (C, C-9), 135.0 (CH, C-5), 126.2 (CH, C-4), 125.9 (CH, C-10), 100.8 (CH, C-1′), 85.5 (CH, C-8), 78.2 (CH, C-11), 74.3 (CH, C-2″), 73.8 (CH, C-3), 73.1 (CH, C-3′), 72.3(CH, C-5′), 71.7 (CH, C-2′), 69.4 (CH_2, C-19), 68.5 (CH, C-4′), 67.3 (CH_2, C-1), 61.3 (CH_2, C-6′), 51.3 (CH, C-2), 32.9 (CH_2, C-12), 32.2 (CH_2, C-3″), 31.9 (CH_2, ω–2), 30.6–29.5 (several CH_2, alkyl chains), 30.4 (CH_2, C-7), 28.9 (CH_2, C-6), 25.3 (CH_2, C-4″), 23.1 (CH_2, ω–1), 20.6–19.9 (several CH_3, acetyl Me groups), 14.3 (CH_3, ω). ^{13}C NMR of **2b** ($CDCl_3$): same signals as for compound **2a**, except for δ 136.0 (C, C-9), 125.4 (CH, C-10), 85.3 (CH, C-8), 78.4 (CH, C-11), 69.5 (CH_2, C-19), 33.3 (CH_2, C-12).

4.2.3. Compounds 2c–2d (inseparable mixture). Colorless oil. ESIMS (positive ion mode, MeOH) *m/z* 1176, 1190, and 1204 ([M+Na]$^+$ series). ^{1}H NMR of **2c** ($CDCl_3$): δ 6.48 (1H, d, J = 9.2 Hz, NH-2), 5.78 (1H, br.s, H-10), 5.74 (2H, s, H-4 and H-5), 5.54 (1H, m, H-3), 5.34 (1H, t, J = 9.8 Hz, H-3′), 5.24 (1H, t, J = 9.8 Hz, H-4′), 5.23 (overlapped, H-2″), 5.14 (1H, dd, J = 9.8 and 7.9 Hz, H-2′), 4.74 (2H, br. s, H2-19), 4.69 (1H, m, H-11), 4.54 (1H, m, H-2), 4.47 (1H, br. dd, J = 9.1 and 4.5 Hz, H-8), 4.22 (1H, dd, J = 12.5 and 4.0 Hz, H-6′a), 4.12 (1H, d, J = 7.9 Hz, H-1′), 4.08 (1 H, dd, J = 12.5 and 2.2 Hz, H-6′b), 3.77 (1H, dd, J = 10.3 and 3.7 Hz, H-1a), 3.45 (1H, dd, J = 10.3 and 4.4 Hz, H-1b), 3.21 (1H, ddd, J = 9.8, 4.0, and 2.2 Hz, H-5′), 2.19 (1H, m, H-6a), 2.04 (1H, m, H-6b), 2.00 (3H, s, Ac), 1.96 (1H, m, H-3″), 1.83 (3H, s, Ac), 1.81 (3H, s, Ac), 1.79 (3H, s, Ac), 1.66 (overlapped, H-7a), 1.67 (3H, s, Ac), 1.65 (3H, s, Ac), 1.60 (overlapped, H-12a), 1.45(overlapped, H-4″), 1.44 (overlapped, H-7b), 1.41 (overlapped, H-12b), 1.32 (broad band, alkyl chain protons), 0.90 (6H, t, J = 7.0, terminal Me groups). ^{1}H NMR of **2d** ($CDCl_3$): same signals as for compound **2c**, except for δ 5.79 (1H, br.s, H-10), 4.82 (1H, br. d, J = 15.8 Hz, H-19a), 4.60 (1H, br. d, J = 15.8 Hz, H-19b), 4.52 (overlapped, H-11), 4.45 (1H, br. dd, J = 9.0 and 4.5 Hz, H-8), 1.76 (overlapped, H-12a), 1.48 (overlapped, H-12b). ^{13}C NMR of **2c** ($CDCl_3$): δ 170.6 (C, C-1″), 170.5-169.1 (several C, acetyl CO groups), 136.6 (C, C-9), 132.8 (CH, C-5), 127.1 (CH, C-4), 125.8 (CH, C-10), 100.7 (CH, C-1′), 84.7 (CH, C-8), 78.2 (CH, C-11), 74.4 (CH, C-2″), 73.0 (CH, C-3′), 72.9 (CH, C-3), 72.3(CH, C-5′), 71.7 (CH, C-2′), 69.4 (CH_2, C-19), 68.5 (CH, C-4′), 67.2 (CH_2, C-1), 61.6 (CH_2, C-6′), 51.8 (CH, C-2), 32.9 (CH_2, C-12), 32.2 (CH_2, C-3″), 31.9 (CH_2, ω–2), 30.7 (CH_2, C-7), 30.6–29.5 (several CH_2, alkyl chains), 28.7 (CH_2, C-6), 25.6 (CH_2, C-4″), 23.1 (CH_2, ω–1), 20.7-20.1 (several CH_3, acetyl Me groups) , 14.3 (CH_3, ω). ^{13}C NMR of **2d** ($CDCl_3$): same signals as for compound **2c**, except for δ 136.4 (C, C-9), 125.2 (CH, C-10), 84.5 (CH, C-8), 78.5 (CH, C-11), 69.5 (CH_2, C-19), 33.5 (CH_2, C-12).

4.3. Deacetylation of compound 1b

Compound **1b** (3.0 mg) was dissolved in 950 µl of MeOH, and 50 µl of a 0.4 M solution of MeONa in MeOH was added. The reaction was allowed to proceed for 18 h at 25 °C, then the reaction mixture was dried under nitrogen and the residue partitioned between water and chloroform. After removal of the solvent, the organic layer gave 2.1 mg of the native glycosphingolipid **1a**.

4.3.1. Corrugoside (1a). Colorless amorphous solid, $[\alpha]_D^{25}$ −5.7 (c = 0.5 in MeOH). ESIMS (positive ion mode, MeOH) *m/z* 1192, 1206 and 1220 ([M+Na]$^+$ series). RESI-MS (positive ion mode, MeOH) *m/z* 1192.7918 ([M + Na]$^+$, $C_{60}H_{115}NNaO_{20}^+$ gives 1192.7910). ^{1}H NMR (pyridine-d_5): δ 8.59 (1H, d, J = 9.0 Hz, 2-NH), 7.64 (1H, d, J = 3.9 Hz, 2^{IV}-OH), 6.95 (1H, d, J = 3.7 Hz, 4‴-OH), 6.92 (1H, br. s, 3‴-OH), 6.65 (1H, br. s, 3-OH), 6.62 (1H, br. s, 6′-OH), 6.60 (1H, br. s, 6″-OH), 6.52 (2H, br. s, 4′-OH and 4″-OH), 6.19 (1H,

d, J = 6.1 Hz, 3″-OH), 6.04 (1H, br. s, 6‴-OH), 6.01 (1H, br. s, 3′-OH), 5.81 (1H, d, J = 3.3 Hz, H-1′), 5.80 (overlapped, 4-OH), 5.77 (1H, d, J = 3.6 Hz, H-1″), 5.51 (1H, d, J = 3.8 Hz, H-1‴), 5.17 (1H, m, H-2), 5.07 (1H, m, H-5″), 4.93 (overlapped, H-5‴), 4.84 (1H, dd, J = 10.0 and 3.3 Hz, H-2′), 4.80 (1H, dd, J = 10.1 and 3.6 Hz, H-2″), 4.71 (1H, m, H-3″), 4.67 (1H, br. t, J = 9.2 Hz, H-3‴), 4.58 (overlapped, H-1a), 4.58 (overlapped, H-2^{IV}), 4.55 (overlapped, H-3′), 4.52 (overlapped, H-5′), 4.52 (1H, br. s, H-4″), 4.49 (1H, br. s, H-4′), 4.44 (1H, m, H-6″a), 4.41 (overlapped, H-1b), 4.39 (overlapped, H-3), 4.39 (overlapped, H-6′a), 4.37 (overlapped, H-6‴a), 4.33 (overlapped, H-6′b), 4.31 (overlapped, H-6‴b), 4.28 (overlapped, H-4), 4.27 (overlapped, H-6″b), 4.22 (1H, m, H-4‴), 4.12 (1H, m, H-2‴), 2.22 (1H, m, H-5a), 2.13 (1H, m, H-3^{IV}a), 1.94 (1H, m, H-3^{IV}b), 1.87 (2H, m, H-5b and H-6a), 1.73 (1H, m, H-4^{IV}a), 1.64 (1H, m, H-6b and H-4^{IV}b), 1.25 (large band, alkyl chains), 0.86 (*n*- and *iso*-chain Me groups); ^{13}C NMR (pyridine-d_5): δ 170.7 (C, C-1^{IV}), 98.5 (CH, C-1‴), 98.1 (CH, C-1′), 97.1 (CH, C-1″), 77.1 (CH, C-2′), 75.7 (CH, C-2″), 75.5 (CH, C-3), 75.1 (CH, C-3‴), 73.8 (CH, C-5‴), 73.6 (CH, C-2‴), 72.6 (CH, C-5′), 72.5 (CH, C-4), 72.5 (CH, C-5″), 72.3 (CH, C-2^{IV}), 71.4 (CH, C-4‴), 71.0 (CH, C-4″), 70.7 (CH, C-4′), 69.4 (CH, C-3′), 69.0 (CH, C-3″), 66.9 (CH_2, C-1), 62.5 (CH_2, C-6″), 62.4 (CH_2, C-6′), 62.2 (CH_2, C-6‴), 51.2 (CH, C-2), 35.4 (CH_2, C-3^{IV}), 33.5 (CH_2, C-5), 32.0 (CH_2, *n*-chain ω–2 CH_2 groups), 30.5-29.5 (several CH_2, alkyl chains), 26.4 (CH_2, C-6), 25.7 (CH_2, C-4^{IV}), 22.8 (CH_2, *n*-chain ω–1 CH_2 groups), 22.7 (CH_3, *iso*-chain Me groups), 14.0 (CH_3, *n*-chain Me groups); Composition in fatty acids: Table 2. Composition in sphinganines: Table 3.

4.4. Degradation analysis of compound 1a

4.4.1. Methanolysis of 1a. Compound **1a** (100 μg) was dissolved in 500 μL of 1 M HCl in 91% MeOH and the obtained solution was kept for about 12 h at 80 °C in a sealed tube. The reaction mixture was dried under nitrogen, and partitioned between $CHCl_3$ and H_2O/MeOH (8:2). The aqueous layer was concentrated to give a mixture of methyl glycosides (fraction A), whereas the organic layer contained a mixture of α-hydroxyacid methyl esters and sphinganines and sphinganines (fraction B).

4.4.2. Methyl tetra-*O*-benzoyl-α-D-glucopyranoside (4). D-Glucose (2.0 mg) was subjected to acidic methanolysis as described above. The resulting methyl glycosides were benzoylated with benzoyl chloride (50 μL) in pyridine (500 μL) at 25 °C for 16 h. The reaction was then quenched with MeOH, and after 30 min was dried under nitrogen. Methyl benzoate was removed by keeping the residue under vacuum for 24 h with an oil pump. The residue was purified by HPLC (column: Luna SiO_2, 5 μm; eluent: *n*-hexane/*i*-PrOH 99:1, flow 1 mL/min, UV dedector), affording the glycoside **4** (t_R = 8.0 min): ^{1}H NMR ($CDCl_3$): δ 3.49 (3H, s, OMe), 4.03 (1H, m, H-5), 4.49 (1H, dd, J = 12.0 and 5.4 Hz, H-6b), 4.61 (1H, dd, J = 12.0 and 3.1 Hz, H-6a), 5.25 (1H, d, J = 3.7, H-1), 5.30 (1H, dd, J = 9.8 and 3.7 Hz, H-2), 5.68 (1H, t, J = 9.8 Hz, H-4), 6.19 (1H, t, J = 9.8, H-3), 7.55–7.24 (12H, overlapping signals, benzoyl protons), 7.80 (2H, t, J = 8.1 Hz, benzoyl ortho protons), 7.94 (2H, d, J = 8.1 Hz, benzoyl ortho protons), 7.88 (2H, d,J = 8.1 Hz, benzoyl ortho protons), 8.00 (2H, d, J = 8.1 Hz, benzoyl ortho protons); CD (MeCN): λ_{max} = 236 nm ($\Delta\varepsilon$ = +11), 220 nm ($\Delta\varepsilon$ = −1).

4.4.3. Absolute stereochemistry of methyl glycosides from compound 1a. Fraction A from methanolysis of compound **1a** was benzoylated with benzoyl chloride (20 μL) in pyridine (200 μL) at 25 °C for 16 h. The reaction was then quenched with MeOH, and after 30 min was dried under nitrogen. Methyl benzoate was removed by keeping the residue under vacuum for 24 h with an oil pump. The residue was purified by HPLC (column: Luna SiO_2; eluent: 5 μm; *n*-hexane/*i*-PrOH 99:1, flow 1 mL/min). The chromatogram contained two peaks, which were identified as methyl tetra-*O*-benzoyl-α-D-galactopyranoside (**5**) (t_R = 8.3 min) and methyl tetra-*O*-benzoyl-α-D-glucopyranoside (**4**) (t_R = 8.0 min) by a comparison of their retention times, ^{1}H NMR spectra and CD spectra with those of the authentic samples prepared, respectively, from D-galactose[2] and D-glucose.

4.4.4. Analysis of fatty acid methyl esters. Fraction B from methanolysis of compound 1a was analyzed by GLC-MS and its components identified by a comparison of their retention times and mass spectra with those of authentic samples. The results are compiled in Table 2.

4.4.5. Analysis of fraction B. Fraction B from methanolysis of compounds **1a** was benzoylated as described above, and the crude of reaction was purified by HPLC (column: Luna SiO_2, 5 μm; eluent: *n*-hexane/*i*-PrOH 99:1, flow 1 mL/min). The chromatogram contained two peaks, which were identified as a mixture of homologues benzoylated fatty acid methyl esters (fraction C, t_R = 4.0 min) and a mixture of perbenzoylated sphinganines (fraction D, t_R = 7.2 min) on the basis of their respective ^{1}H NMR spectra.

4.4.5.1. Methyl (*R*)-2-benzoyloxyalkanoate (fraction C, mixture of homologues). ^{1}H NMR ($CDCl_3$): δ 0.87 (ω Me group), 1.25 (large band, alkyl chain), 1.99 (2H, m, H_2-3), 3.78 (3H, s, OMe), 5.23 (1H, t, J = 6.0 Hz, H-2), 7.44 (2H, t, J = 7.6 Hz, benzoyl meta protons), 7.58 (1H, t, J = 7.5 Hz, benzoyl para proton), 8.10 (2H, d, J = 8.0 Hz, benzoyl ortho protons); CD (MeCN): λ_{max} = 230 nm ($\Delta\varepsilon$ = −4).

4.4.5.2. (2*S*, 3*S*, 4*R*)-1,3,4-*O*-Benzoyl-2-benzamidoamino-1,3,4-alkanetriol (fraction D, mixture of homologues). CD (MeCN): λ_{max} = 233 nm ($\Delta\varepsilon$ = −7), 220 nm ($\Delta\varepsilon$ = +1); the ^{1}H NMR spectrum was identical (apart from the methyl region) to that of an authentic sample of D-*ribo*-phytosphingosine perbenzoate.[2]

4.4.6. Oxidative cleavage and GC–MS analysis of sphinganines. Fraction D was debenzoylated by acidic methanolysis as described above and subjected to oxidative cleavage with $KMnO_4$/$NaIO_4$ as described,[12] and the resulting carboxylic acids were methylated with

CH_2N_2. The obtained esters were analyzed by GC–MS, and the results are compiled in Table 3, expressed in terms of original sphinganines.

4.5. Immunostimulatory activity of corrugoside (1a)

CD1d presentation of lipid antigens to NKT cells was detected using the murine NKT cell hybridoma DN32.D3 that expresses the semi-invariant Vα14Jα18/Vβ8 TCR.[13] Hybridoma cells were cultured in RPMI supplemented with 10% FCS, 2 mM L-glutamine, 20 mM HEPES, and non-essential amino acids. Dendritic cells from C57BL/6 mice were generated in in vitro bone marrow cultures in the presence of GM-CSF[14] and were used as antigen presenting cells. Dendritic cells (104/well) were pulsed with serial dilutions of lipid antigen for 4 h in 96-well round bottom plates. Cells were washed three times before five times 104 DN32.D3 cells were added per well. Supernatant was collected after 24 h and stored at −80 °C until analysis. Interleukin-2 production in supernatants was determined in a bioassay using the [^{3}H]thymidine incorporation of an IL-2 dependent NK cell line as readout.

Acknowledgments

The authors are very grateful to Prof. J.R. Pawlik, University of North Carolina at Wilmington, for inviting them to participate to the third 'Pawlik Expedition' under the National Science Foundation project grant entitled 'Assessing the chemical defenses of Caribbean Invertebrates, during which the material was collected, and Prof. Sven Zea (Universidad Nacional de Colombia) for identifying the sponge. Mass and NMR spectra were recorded at the 'Centro di Servizi Interdipartimentale di Analisi Strumentale, Università di Napoli 'Federico II'. The assistance of the staff is gratefully acknowledged. L.T. is supported by NIH Grants AI053725 and AI070390.

Supplementary data

Supplementary data associated with this article can be found, in the online version, at doi:10.1016/j.bmc.2007.10.098.

References and notes

1. Part 17 Costantino, V.; Fattorusso, E.; Imperatore, C.; Mangoni, A. *J. Nat. Prod.* **2006**, *69*, 73.
2. Costantino, V.; Fattorusso, E.; Imperatore, C.; Mangoni, A. *J. Org. Chem.* **2004**, *69*, 1174.
3. Kawano, T.; Cui, J.; Koezuka, Y.; Toura, I.; Kaneko, Y.; Motoki, K.; Ueno, H.; Nakagawa, R.; Sato, H.; Kondo, E.; Koseki, H.; Taniguchi, M. *Science* **1997**, *278*, 1626.
4. Bendelac, A.; Savage, P. B.; Teyton, L. *Annu. Rev. Immunol.* **2007**, *25*, 297.
5. Tupin, E.; Kinjo, Y.; Kronenberg, M. *Nat. Rev. Microbiol.* **2007**, *5*, 405.
6. Laroche, M.; Imperatore, C.; Grozdanov, L.; Costantino, V.; Mangoni, A.; Hentschel, U.; Fattorusso, E. *Marine Biol.* **2007**, *151*.
7. Costantino, V.; Fattorusso, E.; Imperatore, C.; Mangoni, A. *Eur. J. Org. Chem.* **2005**, 368.
8. Costantino, V.; Fattorusso, E.; Imperatore, C.; Mangoni, A. *Eur. J. Org. Chem.* **2003**, 1433.
9. Grossi, V.; Rontani, J-F. *Tetrahedron Lett.* **1995**, *36*, 3141.
10. Prigozy, T. I.; Naidenko, O.; Qasba, P.; Elewaut, D.; Brossay, L.; Khurana, A.; Natori, T.; Koezuka, Y.; Kulkarni, A.; Kronenberg, M. *Science* **2001**, *291*, 664.
11. Jin, W.; Rinehart, K. L.; Jares-Erijman, E. A. *J. Org. Chem.* **1994**, *59*, 144.
12. Costantino, V.; Fattorusso, E.; Mangoni, A.; Di Rosa, M.; Ianaro, A.; Maffia, P. *Tetrahedron* **1996**, *52*, 1573.
13. Park, S. H.; Roark, J. H.; Bendelac, A. *J. Immunol.* **1998**, *160*, 3128.
14. Inaba, K.; Inaba, M.; Romani, N.; Aya, H.; Deguchi, M.; Ikehara, S.; Muramatsu, S.; Steinman, R. M. *J. Exp. Med.* **1992**, *176*, 1693.